Ligand Substitution Reactions of $W_6S_8L_6$ with Tricyclohexylphosphine (L = 4-*tert*-Butylpyridine or *n*-Butylamine): ^{31}P NMR and Structural Studies of $W_6S_8(PCy_3)_n$(4-*tert*-butylpyridine)$_{6-n}$ ($0 < n \leq 6$) Complexes

Song Jin, D. Venkataraman, and Francis J. DiSalvo*

Baker Laboratories, Department of Chemistry and Chemical Biology, Cornell University, Ithaca, New York 14853

Received December 14, 1999

The substitution reactions by bulky tricyclohexylphosphine (PCy_3) ligands on $W_6S_8L_6$ (L = 4-*tert*-butylpyridine or *n*-butylamine) clusters were investigated to prepare clusters with mixed axial ligands for low-dimensional cluster linking. When 4−6 equiv of PCy_3 are used to react with W_6S_8(4-*tert*-butylpyridine)$_6$ (**4**) in THF, *cis*-$W_6S_8(PCy_3)_4$(4-*tert*-butylpyridine)$_2$ (**1**) is preferentially formed. But when starting with W_6S_8(*n*-butylamine)$_6$ (**2**), only $W_6S_8(PCy_3)_6$ (**3**) is produced with 6 equiv of PCy_3. Other conditions with fewer equivalents of PCy_3 led to mixtures of partially substituted complexes in the $W_6S_8L_{6-n}(PCy_3)_n$ ($0 \leq n \leq 6$, L = 4-*tert*-butylpyridine or *n*-butylamine) series. A significantly distorted structure for **1** helps to explain its preferential formation. ^{1}H NMR spectra were collected for clusters **1** and **2** and ^{31}P NMR spectra for **1** and W_6S_8(4-*tert*-butylpyridine)$_{6-n}(PCy_3)_n$ complexes. P−P coupling through P−W−W−P is reported for the first time in octahedral metal clusters and shown to be very useful in identifying nearly all the $W_6S_8L_{6-n}(PR_3)_n$ complexes and their stereoisomers in the mixtures even before individual species are isolated.

Introduction

Extensive attention has been drawn to chalcogenide metal clusters,[1−4] especially the group 6 octahedral $M_6Q_8^{2-4}$ (M = Cr,[5−11] Mo,[12−17] W;[18−24] Q = S, Se, Te) metal clusters with eight chalcogenide atoms as face-capped bridging atoms, because of the well-known superconducting Chevrel phases[25] discovered nearly two decades ago as well as their catalytic activity.[26,27] Following the first successful preparation and isolation of molecular $M_6Q_8L_6$ clusters in solution more than 10 years ago by Saito and co-workers,[17,18] we focused on these molecular clusters aiming at constructing novel solid-state materials from solutions using clusters as building blocks.

The electronic structure of these octahedral group 6 chalcogenide metal clusters and projected solid-state cluster networks built from them is of particular interest. Extended Hückel calculations, done in collaboration with R. Hoffmann, showed that extended structures built using these clusters and ditopic ligands with extended π systems allow electronic communication through the networks.[28] After we achieved a high-yield synthesis of W_6S_8(4-tbp)$_6$ (**4**) (4-tbp = 4-*tert*-butylpyridine) molecular cluster as starting material,[20] we have pursued several

* To whom correspondence should be addressed. E-mail: fjd3@cornell.edu.

(1) Reviews after 1990. (a) Lee, S. C.; Holm, R. H. *Angew. Chem., Int. Ed. Engl.* **1990**, *29*, 840−56. (b) Bencini, A.; Midollini, S. *Coord. Chem. Rev.* **1992**, *120*, 87−136. (c) Holm, R. H. *Adv. Inorg. Chem.* **1992**, *38*, 1−71. (d) Roof, L. C.; Kolis, J. W. *Chem. Rev.* **1993**, *93*, 1037. (e) Dance, I.; Fisher, K. *Prog. Inorg. Chem.* **1994**, *41*, 637−803. (f) Perrin, C. *J. Alloys Compd.* **1997**, *262−263*, 10−21. (g) Saito, T. *J. Chem. Soc., Dalton Trans.* **1999**, 97−106.
(2) Prokopuk, N.; Shriver, D. F. *Adv. Inorg. Chem.* **1998**, *46*, 1−49.
(3) Saito, T. In *Early Transition Metal Clusters with π-Donor Ligands*; Chisholm, M. H., Ed.; VCH Publishers: Weinheim, Germany, 1995.
(4) Saito, T. *Adv. Inorg. Chem* **1997**, *44*, 45−91.
(5) Hessen, B.; Siegrist, T.; Palstra, T.; Tanzler, S. M.; Steigerwald, M. L. *Inorg. Chem.* **1993**, *32*, 5165−5169.
(6) Kamiguchi, S.; Imoto, H.; Saito, T. *Chem. Lett.* **1996**, 555−556.
(7) Kamiguchi, S.; Imoto, H.; Saito, T.; Chihara, T. *Inorg. Chem.* **1998**, *37*, 6852−6857.
(8) Saito, T.; Imoto, H. *Bull. Chem. Soc. Jpn.* **1996**, *69*, 2403−2417.
(9) Tsuge, K.; Imoto, H.; Saito, T. *Bull. Chem. Soc. Jpn.* **1996**, *69*, 627−636.
(10) Amari, S.; Imoto, H.; Saito, T. *Chem. Lett.* **1997**, 967−968.
(11) Amari, S.; Imoto, H.; Saito, T. *J. Chin. Chem. Soc. (Taipei)* **1998**, *45*, 445−450.
(12) Hilsenbeck, S. J.; McCarley, R. E.; Goldman, A. I. *Chem. Mater.* **1995**, *7*, 499−506.
(13) Hilsenbeck, S. J.; Young, V. G., Jr.; McCarley, R. E. *Inorg. Chem.* **1994**, *33*, 1822−1832.
(14) McCarley, R. E.; Hilsenbeck, S. J.; Xie, X. *J. Solid State Chem.* **1995**, *117*, 269−274.
(15) Mizutani, J.; Amari, S.; Imoto, H.; Saito, T. *J. Chem. Soc., Dalton Trans.* **1998**, 819−824.
(16) Saito, T.; Yamamoto, N.; Nagase, T.; Tsuboi, T.; Kobayashi, K.; Yamagata, T.; Imoto, H.; Unoura, K. *Inorg. Chem.* **1990**, *29*, 764−770.
(17) Saito, T.; Yamamoto, N.; Yamagata, T.; Imoto, H. *J. Am. Chem. Soc.* **1988**, *110*, 1646−1647.
(18) Saito, T.; Yoshikawa, A.; Yamagata, T. *Inorg. Chem.* **1989**, *28*, 3588−3592.
(19) Ehrlich, G. M.; Warren, C. J.; Vennos, D. A.; Ho, D. M.; Haushalter, R. C.; DiSalvo, F. J. *Inorg. Chem.* **1995**, *34*, 4454−4459.
(20) Venkataraman, D.; Rayburn, L. L.; Hill, L. I.; Jin, S.; Malik, A.-S.; Turneau, K. J.; DiSalvo, F. J. *Inorg. Chem.* **1999**, *38*, 828−830.
(21) Zhang, X.; McCarley, R. E. *Inorg. Chem.* **1995**, *34*, 2678−2683.
(22) Xie, X. B.; McCarley, R. E. *Inorg. Chem.* **1995**, *34*, 6124−6129.
(23) Xie, X. B.; McCarley, R. E. *Inorg. Chem.* **1996**, *35*, 2713−2714.
(24) Xie, X.; McCarley, R. E. *Inorg. Chem.* **1997**, *36*, 4011−4016.
(25) (a) Chevrel, R.; Sergent, M.; Prigent, J. *J. Solid State Chem.* **1971**, *110*, 515−519. (b) Chevrel, R.; Sergent, M. *Topics in Current Physics*; Fischer, O., Maple, M. B., Eds.; Springer-Verlag: Heidelberg, 1982; Vol. 32, Chapter 2.
(26) (a) McCarty, K. F.; Anderegg, J. W.; Schrader, G. L. *J. Catal.* **1985**, *93*, 375−387. (b) Kareem, S. A.; Miranda, R. *J. Mol. Catal.* **1989**, *53*, 275−283. (c) Ekman, M. E.; Anderegg, J. W.; Schrader, G. L. *J. Catal.* **1989**, *117*, 246−257.
(27) (a) Hilsenbeck, S. J.; McCarley, R. E.; Thompson, R. K.; Flanagan, L. C.; Schrader, G. L. *J. Mol. Catal. A* **1997**, *122*, 13−24. (b) Hilsenbeck, S. J.; McCarley, R. E.; Goldman, A. I.; Schrader, G. L.; Glenn, L. *Chem. Mater.* **1998**, *10*, 125−134.
(28) Malik, A.-S. Ph.D. Thesis, Cornell University, Ithaca, NY, 1998.

10.1021/ic991426l CCC: $19.00
Published on Web 06/07/2000

directions toward the final goal of extended structures based on clusters. (1) Oxidize some or all of the $W_6S_8L_6$ clusters by one or more electrons to induce electronic conduction in linked networks.[28] Oxidation behavior will be reported in a separate publication. (2) Replace the monodentate ligands (L) on the cluster with π-conjugated ditopic ligands such as 4,4′-bipyridine so extended 3-D networks with clusters as building block can be formed. The biggest obstacle in this direction is that insoluble amorphous products are typically formed. (3) Make clusters with mixed axial ligands that have different binding energies or labilities so that low-dimensional extended networks can be formed by replacing the thermodynamically less favorable or labile ligands with ditopic ligands while leaving the thermodynamically more favorable or inert ligands unaffected. This might not only offer us a variety of extended structures but also help to circumvent the insolubility problem mentioned above. Since the last two directions only involve axial ligand substitution reactions, we are probing the axial ligand coordination chemistry of W_6S_8 clusters in order to reach the above goals. Such substitution chemistry is the subject of this report.

The controlled low-dimensional linking of clusters is conceptually analogous to the self-assembly of inorganic metal ions and organic multitopic ligands in supramolecular inorganic chemistry[29] that has recently attracted considerable attention. Conceptually, single metal ion coordination centers in these self-assembled networks can just be replaced by the six-coordinated metal clusters. This chemistry of multinuclear cluster cores utilized in place of single metal centers has been envisioned and partially exemplified in the $[Re_6Q_8(PEt_3)_{6-n}X_n]^{2-n}$ (Q = S, Se; X = Br^-, I^-; $1 < n \leq 6$) system by Holm and co-workers.[30,31] However, the HOMO symmetry in the $\{Re_6Q_8\}^{2+}$ clusters is not suitable for electronic conduction. Further, the axial ligand coordination chemistry of *neutral* group 6 chalcogenide octahedral clusters has not been explored so far, as opposed to the relatively established axial ligand exchange studies on *anionic* group 6 halide octahedral clusters[32] and *cationic* $\{Re_6Q_8\}^{2+}$ clusters.[30,31,33]

We previously showed that phosphine ligands (PR_3) are the most substitutionally inert ligands when bound to a W_6S_8 cluster[20] and thus are the natural candidates for blocking the selected positions on W_6S_8 cluster. However, we observed a wide distribution of species when triethylphosphine (PEt_3) replaces other ligands. Subsequently, bulky tricyclohexylphosphine (PCy_3, Cy = cyclohexyl) was utilized in the hope of generating partially substituted cluster complexes $W_6S_8L_{6-n}(PCy_3)_n$ ($0 < n < 6$). Reported here are the syntheses, some crystal structures of the resulting complexes of (partial) ligand substitution by PCy_3, and ^{31}P NMR spectra of these complexes, which were very useful in identifying them. We observe P−P coupling through the octahedral clusters and use that coupling to distinguish different compositions and isomers in the series $W_6S_8L_{6-n}(PR_3)_n$.

Experimental Section

General. W_6S_8(4-*tert*-butylpyridine)$_6$ cluster was synthesized according to our improved procedure.[20] All other reagents were of commercial origin. Acetonitrile and *n*-butylamine were dried with 4 Å molecular sieves and potassium hydroxide, respectively, and were degassed and distilled under reduced pressure. THF, diethyl ether, and benzene were treated with sodium wire and distilled under reduced pressure. All others were used as received. All the reagents and products were stored in a glovebox filled with argon. All the operations were carried out in the glovebox unless otherwise stated. The "reaction bomb" used below is a thick-walled glass vessel (i.d. = 1 in.; thickness = $^1/_8$ in.) with a Teflon valve equipped with a Teflon stir bar.

^1H and ^{13}C NMR spectra were obtained in C_6D_6 solution unless otherwise noted using an IBM/Bruker AF-300 or a Varian VXR-400 instrument with no ^{31}P decoupling and were internally referenced to residual solvent resonance. ^{31}P NMR spectra were obtained using a Varian VXR-400 instrument at 162 MHz with 85% H_3PO_4 as external standard and with ^1H decoupling unless otherwise noted. Microprobe elemental analyses by EDAX (energy dispersive analysis by X-rays) were performed on a JEOL 8900R using the vendor-supplied SQ package for standardless semiquantitative elemental analysis. Powder X-ray diffraction was done on a Scintag XDS2000 diffractometer.

Typical Synthesis of *cis*-$W_6S_8(PCy_3)_4$(4-*tert*-butylpyridine)$_2$ (1). W_6S_8(4-*tert*-butylpyridine)$_6$ (1.00 g, 0.461 mmol) and tricylcohexylphosphine (PCy_3) (0.646 g, 2.30 mmol; cluster/PCy_3 ratio = $^1/_5$) were loaded into a reaction bomb along with 15 g of THF. The reaction vessel was taken out of the glovebox and heated at 100 °C shielded from light for 48 h. Within less than an hour, the initial brick-red slurry turned into a dark-red clear solution. Then some red precipitate formed in a few hours. After the solution was cooled, the precipitate was filtered and washed with THF repeatedly, then washed with Et_2O. After drying in vacuo, the fine red powder of the final products of *cis*-$W_6S_8(PCy_3)_4$(4-tbp)$_2$ (**1**) weighed 1.24 g (98% yield).

Cluster **1** prepared in this way is soluble in 4-tbp and benzene, but it takes some time for the cluster to dissolve in benzene. ^1H NMR: δ 9.62 (d, α-H), 6.89 (d, β-H), 3.64−3.49, 2.74−2.31, 2.13−1.82, 1.82−1.66, 1.66−1.33, 1.48 (all broad bands, H on PCy_3), 0.86 (s, Me). $^{31}P\{^1H\}$ NMR: δ 6.297 (t, $^3J_{p-p}$ = 2.4 Hz), 4.261 (t, $^3J_{p-p}$ = 2.4 Hz); satellite peaks (all broad) 6.86−6.96, 5.62−5.72 ($^1J_{w-p}$ = 205 Hz), 4.86−4.96, 3.58−3.68 ($^1J_{w-p}$ = 206 Hz).

Other Reactions of PCy_3 with W_6S_8(4-tbp)$_6$ (4). Different ratios of the W_6S_8(4-tbp)$_6$ cluster to PCy_3 were used as reactants with other conditions being identical. Results are the following (cluster:PCy_3 ratio).

1:2. An amount of 100 mg of **4** was used, and no powder was filtered out. The dark-red solution was a mixture of $W_6S_8(PCy_3)_n(tbp)_{6-n}$ ($0 \leq n \leq 4$) by NMR. $^{31}P\{^1H\}$ NMR (spectrum available in Supporting Information): δ 13.646 (s), singlet satellites at 14.273 and 13.018 ($^1J_{w-p}$ = 203 Hz); 11.404 (s with shoulders), doublet satellites at 12.047 and 10.777 ($^1J_{w-p}$ = 205 Hz); 11.012 (s), satellites unrecognizable; 9.216 (s with shoulders), triplet satellites at 9.841 and 8.563 ($^1J_{w-p}$ = 207 Hz); 8.635 (d, J_{p-p} = 2.4 Hz) and 7.852 (t, J_{p-p} = 2.4 Hz); 6.297 (t, J_{p-p} = 2.4 Hz) and 4.261 (t, J_{p-p} = 2.4 Hz).

1:3. An amount of 300 mg of **4** was used, and 97 mg of red powder was filtered out of a dark-bloody-red solution. The powder was found to be *cis*-$W_6S_8(PCy_3)_4$(4-tbp)$_2$ by NMR and powder XRD. Yield: 26% based on **4**, 34% based on PCy_3.

1:4. An amount of 150 mg of **4** was used, and 142 mg of red powder, which was identified as *cis*-$W_6S_8(PCy_3)_4$(4-tbp)$_2$ by NMR and powder XRD, was acquired. Yield: 75%.

1:6. An amount of 300 mg of **4** was used, and 350 mg of red powder, which was identified as *cis*-$W_6S_8(PCy_3)_4$(4-tbp)$_2$ by NMR and powder XRD, was acquired. Yield: 92%.

1:12. A turbid brownish-green suspension solution resulted after 1 day of heating. The yellowish green powder filtered out of a light-red filtrate was identified as $W_6S_8(PCy_3)_6$ (**3**) cluster by powder XRD. The

(29) (a) Lehn, J.-M. *Angew. Chem., Int. Ed. Engl.* **1990**, *29*, 1304. (b) Lehn, J.-M. *Pure Appl. Chem.* **1994**, *66*, 1961−1966. (c) Lehn, J.-M. *Supramolecular Chemistry: Concepts and Perspectives*; VCH publishers: Weinheim, Germany, 1995. (d) Moore, J. S.; Lee, S. *Chem. Ind.* **1994**, 556−560. (e) Robson, R.; Abrahams, B. F.; Batten, S. R.; Gable, R. W.; Hoskins, B. F.; Liu, J. In *ACS Symposium Series*; Bein, T., Ed.; American Chemical Society: Washington, D.C., 1992; Vol. 499. (f) Zaworotko, M. J. *J. Chem. Soc. Rev.* **1994**, *23*, 283−288.

(30) Willer, M. W.; Long, J. R.; McLauchlan, C. C.; Holm, R. H. *Inorg. Chem.* **1998**, *37*, 328−333.

(31) Zheng, Z.; Gray, T. G.; Holm, R. H. *Inorg. Chem.* **1999**, *38*, 4888−4895.

(32) (a) See ref 2. (b) Preetz, W.; Peters, G.; Bublitz, D. *Chem. Rev.* **1996**, *96*, 977−1025. (c) Our work. Ehrlich, G. M.; Deng, H.; Hill, L. I.; Steigerwald, M. L.; Squattrito, P. J.; DiSalvo, F. J. *Inorg. Chem.* **1995**, *34*, 2480−2482. Ehrlich, G. M.; Warren, C. J.; Haushalter, R. C.; DiSalvo, F. J. *Inorg. Chem.* **1995**, *34*, 4284−4286.

(33) (a) Zheng, Z.; Long, J. R.; Holm, R. H. *J. Am. Chem. Soc.* **1997**, *119*, 2163−2171. (b) Zheng, Z. P.; Holm, R. H. *Inorg. Chem.* **1997**, *36*, 5173−5178.

Table 1. Crystallographic Data for *cis*-$W_6S_8(PCy_3)_4$(4-tbp)$_2$ (**1**)·heptane, W_6S_8(*n*-butylamine)$_6$ (**2**), and $W_6S_8(PCy_3)_6$ (**3**)·2 heptane

	1·2 heptane	**2**	**3**·2 heptane
chemical formula	C104 H190 N2 P4 S8 W6	C24 H66 N6 S8 W6	C122 H230 P6 S8 W6
fw	2952.04	1798.41	3242.46
space group	*C*2/*c* (No. 15)	*C*2/*m* (No. 12)	$P\bar{1}$ (No. 2)
a, Å	31.2094(2)	10.0667(11)	15.07290(10)
b, Å	13.1764(2)	17.699(2)	15.25580(10)
c, Å	29.4518(5)	14.374(2)	16.0623(2)
α, deg	90	90	62.1610(10)
β, deg	111.3210(10)	105.171(2)	78.8130(10)
γ, deg	90	90	73.481
V, Å^3	11282.5(3)	2471.8(5)	3123.06(5)
Z	4	2	1
temp, °C	−108 (2)	25 (2)	−108 (2)
λ, Å	0.710 73	0.710 73	0.710 73
ρ_{calcd}, g cm^{-3}	1.738	2.416	1.724
μ, cm^{-1}	63.41	142.64	57.59
R_1[a] ($I > 2\sigma$/all)	0.0365/0.0593	0.0768/0.15400	0.0460/0.0752
wR_2[b] ($I > 2\sigma$/all)	0.0632/0.0704	0.2022/0.2482	0.1201/0.1443

[a] $R_1 = \sum||F_o| - |F_c||/\sum|F_o|$. [b] $wR_2 = [\sum w(F_o^2 - F_c^2)^2/\sum w(F_o^2)^2]^{1/2}$.

solubility property is the same as that of **3**. Microprobe (typical relative experimental error 10%) showed a P to W and S ratio consistent with theoretical values. Observed weight percentages (calculated) were the following: W, 71% (68.6%); S, 19% (16.6%); P, 12% (12.0%).

1:6 Reaction in Benzene. A dark-red clear solution resulted. The solution was pumped to dryness, and the residue was transferred and washed onto a filter paper with THF and Et_2O. The fine red powder acquired was found to contain *cis*-$W_6S_8(PCy_3)_4$(4-tbp)$_2$ (**1**) cluster with minor impurities indicated by ^{1}H and ^{31}P NMR. This powder readily dissolves in benzene. The red-orange filtrate solution was found to be a mixture of complexes $W_6S_8(PCy_3)_{6-n}$(tbp)$_n$ ($0 < n < 6$) by ^{1}H and ^{31}P NMR.

Conversion Reaction of *cis*-$W_6S_8(PCy_3)_4$(4-*tert*-butylpyridine)$_2$ (1). A benzene solution of **1** was sealed in a reaction bomb, taken out, and heated to 100 °C for 3 days without apparent change in the appearance. Crystallization efforts of layering heptane on this solution yielded crystals with the same cell constants as described below for *cis*-$W_6S_8(PCy_3)_4$(4-tbp)$_2$·2 heptane. Another crystallization carried out by slowly evaporating the benzene solution gave needle-shaped crystals with different cell constants. The structure solution showed the same *cis*-$W_6S_8(PCy_3)_4$(4-tbp)$_2$ cluster but with different solvents of crystallization (see section on determination of crystal structures).

Another reaction of **1** in C_6D_6 at 100 °C was monitored by quantitative ^{31}P NMR (delay time d1 = 5 s with 90° flip angle) in a NMR tube equipped with a Teflon valve without external standards. The spectrum before the heating was as reported above for *cis*-$W_6S_8(PCy_3)_4$(4-tbp)$_2$. Some new peaks emerged after heating for 1 day (known peaks were used as reference, satellite peaks omitted): δ 9.216 (s); 8.635 (d, $J_{p-p} = 2.4$ Hz), 7.851 (t, $J_{p-p} = 2.4$ Hz); 4.774 (s); −0.045 (d, $J_{p-p} = 2.4$ Hz), −3.454 (quintet, $J_{p-p} = 2.4$ Hz). And integrals of the peaks after 3.5 days (chemical shifts, numbers of P for this peak per cluster) are the following: 3.95 (9.216, 3P), 2.96 (8.635, 2P), 1.29 (7.851, 1P), 36.76 (6.297, 2P), 4.41 (4.774, 4P), 36.87 (4.261, 2P), 10.91 (−0.045, 4P), 2.85 (−3.454, 1P). Integrals after 3.5 days were very close to the above.

Typical Synthesis of W_6S_8(*n*-butylamine)$_6$ (2). A reaction bomb was charged with W_6S_8(4-tbp)$_6$ (1.00 g, 0.461 mmol) and *n*-butylamine (4.0 g, 55 mmol). The reaction vessel was taken out and heated to 100 °C for 3 days. The cluster gradually dissolved into the solution, and a dark-red solution resulted. About 15 mL of acetonitrile was layered onto the solution to afford dark-red crystals in several days. After being filtered out and washed with acetonitrile and Et_2O, the final product **2** weighed 0.57 g (69% yield). ^{1}H NMR in CD_2Cl_2: δ 3.45 (t, 2H on N), 2.99−2.89 (m, 2H on α-C), 1.50 (quintet, 2H on *β*-C), 1.35 (septet, 2H on *γ*-C), 0.91 (t, Me). ^{13}C NMR: δ 50.06 (α-C), 35.68 (*β*-C), 20.03 (*γ*-C), 14.26 (Me).

Synthesis of $W_6S_8(PCy_3)_6$ (3). W_6S_8(*n*-butylamine)$_6$ (**2**) cluster (0.200 g, 0.111 mmol) and PCy_3 (0.187 g, 0.666 mmol; cluster/PCy_3 = 1/6) were loaded into a reaction bomb along with 8 g of THF and heated to 100 °C for 3 days. The yellow-greenish fine precipitate that formed after 1 day was filtered and weighed 0.233 g (yield 68%). After the dark-red filtrate was concentrated to about 2 mL, heptane was layered to afford rod-shaped red crystals suitable for X-ray analysis in 2 weeks. The yellow-greenish powder was found to be the $W_6S_8(PCy_3)_6$ cluster (**3**) from powder XRD and microprobe analysis. When red crystals of $W_6S_8(PCy_3)_6$ are ground, a yellow-greenish powder is produced. The crystals and the greenish powder are slightly soluble in CS_2, sparingly soluble in benzene and THF, and insoluble in other commonly seen solvents.

X-ray Structure Determination. Single-crystal X-ray diffraction data on the following crystals were collected on a Bruker SMART system with a CCD detector. Crystals were mounted on a thin glass fiber using polybutene oil and were immediately cooled in a cold N_2 stream, and the data were collected at 165 K except for the case of W_6S_8(*n*-butylamine)$_6$ (**2**). The structures were solved using SHELXS and refined using full-matrix least-squares method on F_o^2 with SHELXL software packages.[34] Empirical absorption corrections were applied using the SADABS program.[35] The crystallographic data are listed in Table 1.

(a) *cis*-$W_6S_8(PCy_3)_4$(4-*tert*-butylpyridine)$_2$ (1)·2 heptane. Single crystals were grown by layering heptane on the top of the solution of **1** in benzene. A transparent block-shaped red crystal was mounted on the diffractometer. By use of the SMART program, C-centered monoclinic cell constants were found with more than 50 well-centered reflections. Systematic absence conditions suggested the space group *Cc* (No. 9) or *C*2/*c* (No. 15). The structure solution using direct methods in *C*2/*c* revealed correct positions of W and S atoms. Non-hydrogen atoms on the ligands were located using difference Fourier synthesis after least-squares refinements. Further refinements revealed the position of the heptane solvent molecule, of which two terminal C atoms were modeled as being disordered. All the hydrogen atoms were assigned to ideal positions. All the non-hydrogen nonsolvent atoms were refined successfully with anisotropic thermal parameters. The full-matrix least-squares on F_o^2 converged very well with very satisfactory residual *R* values. The residual electron densities were near the W atoms.

(b) *cis*-$W_6S_8(PCy_3)_4$(4-*tert*-butylpyridine)$_2$ (1)·2C_6H_6. An alternative way of growing single crystals was the slow evaporation of the benzene solution of compound **1** in a glovebox to afford needle-shaped crystals when the solution was nearly dry. A well-shaped transparent red crystal was mounted, and primitive monoclinic cell constants were found: $a = 13.1413(2)$ Å, $b = 22.8541(6)$ Å, $c = 20.1462(5)$ Å, and $\beta = 92.735(1)°$. The data collection and integration with the SMART and SAINT programs went well. Systematic absence conditions indicated $P2_1$ (No. 4) as the space group. Structure solution using the direct method revealed the correct positions of W and S atoms. Though with some difficulty, the ligand atoms could be located after the least-squares refinements with difference Fourier synthesis. The connectivity

(34) Sheldrick, G. M. *SHELXL*, ver. 5.03; Siemens Analytical X-ray Instruments Inc.: Madison, WI, 1994.

of the ligand moieties established that the cluster complex is also *cis*-$W_6S_8(PCy_3)_4(4\text{-tbp})_2$. However, the structure refinement of the ligands could not be improved any further and many ghost peaks were encountered around the cluster core. Further scrutiny of the raw reflection frames revealed that the crystal was actually twinned. The TWINNING program (TW)[36] was applied to improve the refinement. With the new data after TW, W and S atoms could be refined anisotropically and solvent benzene molecules were located. But the refinements could not give an acceptable *R* factor ($R_1 = 11.69\%$), and the residual electron densities were still high (16.405 and -7.635 e $Å^{-3}$). Since the connectivity of the ligands on the metal cluster was quite clear already, no additional attempts were made to collect data on possibly better crystals.

(c) W_6S_8(*n*-butylamine)$_6$ (2). Single crystals were grown by recrystallization in *n*-butylamine layered with acetonitrile. A block-shaped dark-red crystal was sealed into a glass capillary together with the mother liquid, and the data were collected at room temperature. A C-centered monoclinic cell was found using the routine program. Three space groups were recommended by the XPREP program on the basis of systematic absences: *C*2/*m* (No. 12), *C*2 (No. 5), and *Cm* (No. 8), with the order of increasing CFOM parameter. Structure solution failed in space group *Cm*, and racemic twins were needed for structure refinements in space group *C*2. The best result was obtained in space group *C*2/*m*. The correct positions for W and S atoms were revealed with direct methods, and other atoms were located in the subsequent cycles of least-squares refinements with Fourier difference maps. Abnormally high thermal parameters were found for the C atoms on restrained butyl ligands. But the attempt to build a disordered model for these butyl groups did not give satisfactory results. H atoms on C and N atoms were assigned to ideal positions. The W and S atoms were refined successfully with anisotropic thermal parameters and no reasonable solvent molecules could be located with most of the residues close to cluster cores. Final refinement converged and gave acceptable *R* factors.

(d) $W_6S_8(PCy_3)_6$ (3)·2 heptane. Single crystals were acquired as described in the preparation section. A block-shaped red transparent crystal was mounted, and triclinic cell constants were found with more than 50 well-centered reflections. A structure solution using the direct methods in $P\bar{1}$ (No. 2) revealed the correct positions of W and S atoms. Difference Fourier synthesis following subsequent least-squares refinements revealed the atoms on ligands gradually. Further refinements revealed the positions of the solvent heptane molecules. The H atoms were assigned to ideal positions. All the nonsolvent non-hydrogen atoms were successfully refined anisotropically. Residual electron densities were mostly near the W atoms.

Thermogravimetric Analysis (TGA). The thermogravimetric analyses (TGA) of the cluster complexes were done on a Seiko TG/DTA 220 thermal analyzer. The samples were loaded onto an aluminum pan and were heated from room temperature to 550 °C at a rate of 20 °C/min under a flow of dinitrogen (60 mL/min).

Results and Discussion

A. Ligand Substitution Reactions of $W_6S_8L_6$ with PCy_3. Our goal was to make the octahedral tungsten sulfide clusters with inert axial ligands at selected positions to be used as precursors in low-dimensional linking reactions. Phosphines are the ligands of choice because they are substitutionally inert, i.e., difficult to exchange with the pyridine-based ligands typically used in linking reactions. They can lock the desired ligand configurations onto the clusters, so we can preferentially replace the more labile (or thermodynamically less favorable) ligands with the ditopic ligands. The concern was how to make the desired clean $W_6S_8(PR_3)_{6-n}L_n$ cluster(s) in high yield because our experiments showed that partial substitution reactions of $W_6S_8(tbp)_6$ cluster with small phosphine ligands such as triethylphosphine gave a wide distribution of all the expected $W_6S_8(tbp)_{6-n}(PEt_3)_n$ complexes. Therefore, we looked into bulky phosphine ligands hoping that the bulkiness of the ligands will drive the desired cluster complex(es) to form.

We chose tricyclohexylphosphine (PCy_3) because it has the largest Tolman cone angle[37] below 180° in the commonly available phosphine ligands (160° based on the statistical survey of crystal structures[38] and 170° based on Tolman's model[37]). Care must be taken in applying the Tolman cone angle concept developed for *single* metal ion complexes to the analogous but much *bigger* W_6S_8 clusters. Steric requirements from the ligands on the clusters are still the ultimate criteria. Therefore, phosphines with more than 180° cone angles (for instance, P(*t*-Bu)$_3$, 182° and P(*o*-Tol)$_3$, 194° [37]) should be avoided because the "fold back" ligand cones can bump into the S on the corners of the square faces of the W_6S_8 cube and decrease the binding strength of these ligands to clusters. Also, the largest ligand (by total volume) should be used if ligand−ligand interaction is desired because the P−P separation is much larger than that of single metal ions. A common choice for bulky phosphine, PPh_3, not only falls short in cone angle (148° by statistics[38] or 145° by Tolman's model[37]) but also has a potential solubility problem based on our experience with $W_6S_8(py)_6$ and $W_6S_8(tbp)_6$ clusters.[19] Thus, PCy_3 became the ligand of choice. On the basis of some simple modeling, it was hoped that only two PCy_3 ligands would replace the 4-tbp ligands on the $W_6S_8(tbp)_6$ cluster in a trans manner to produce *trans*-$W_6S_8(PCy_3)_2(4\text{-tbp})_4$, a good starting material for 2-D linking.

Synthesis of *cis*-$W_6S_8(PCy_3)_4$(4-*tert*-butylpyridine)$_2$ (1). The experimental results of ligand exchange with PCy_3 were surprising. First of all, *cis*-$W_6S_8(PCy_3)_4(4\text{-tbp})_2$ (**1**) cluster is the dominant complex and the easiest to separate in a direct ligand substitution reaction with $W_6S_8(4\text{-tbp})_6$. Second, the cluster with six bulky PCy_3 ligands exists and can be readily made if we start with a labile ligand as in W_6S_8(*n*-butylamine)$_6$ (**3**).

cis-$W_6S_8(PCy_3)_4(4\text{-tbp})_2$ is almost the only complex formed when 5−6 equiv of PCy_3 were used to replace 4-tbp in $W_6S_8(4\text{-tbp})_6$ in THF, and it precipitates out. On the basis of the yields of these powders, only small amounts of other complexes in the $W_6S_8(PCy_3)_{6-n}(4\text{-tbp})_n$ family could be present in the filtrates. Even with 3 equiv of PCy_3, there was still substantial amount of **1** formed—a 34% observed yield assuming all the PCy_3 was used to produce this compound. It is easier to separate **1** in THF as the solvent than in benzene, which can be attributed to the low solubility of *cis*-$W_6S_8(PCy_3)_4(4\text{-tbp})_2$ in THF but comparable solubility of most complexes in benzene.

Why is *cis*-$W_6S_8(PCy_3)_4(4\text{-tbp})_2$ the easiest species to acquire in the substitution of $W_6S_8(tbp)_6$ with PCy_3? First, as shown by the crystal structures, the ligand exchange reactions, and a comparison of TGAs (vide infra), PCy_3, even as bulky as it is, is thermodynamically more favorable than the 4-tbp ligand. Thermodynamically, the PCy_3 ligand has a strong tendency to replace the 4-tbp ligands on the clusters. But the substitution may be stopped by steric hindrance. It was assumed that the balance between these two factors would lead to the formation of *trans*-$W_6S_8(PCy_3)_2(4\text{-tbp})_4$ cluster. The results show that PCy_3 is not bulky enough to stop the substitution at this stage. Instead it goes further and replaces four out of six 4-tbp ligands on the 4-tbp cluster. The conformational flexibility and "intermesh-

(35) Sheldrick, G. M. *SADABS* (the computer program is used by Siemens CCD diffractometers); Institute für Anorganische Chemie der Universität Göttingen: Göttingen, Germany, 1998.
(36) Sparks, R. *TW: TWINNING program*; Bruker Instruments Inc.: Madison, WI, 1998.
(37) Tolman, C. A. *Chem. Rev.* **1977**, *77*, 313−348.
(38) Muller, T. E.; Mingos, D. M. P. *Transition Met. Chem.* **1995**, *20*, 533−539.

ing"[38] of the ligands (see discussion of crystal structures) make the real ligand interaction smaller than suggested by the cone angle and the length of the cyclohexyl group. With four PCy_3 ligands on the W_6S_8 cluster, it's rather easy to argue that the cis configuration is favored over the trans configuration because some strain can be released by distortions in this highly crowded cis structure (see discussion of crystal structure).

The substitution behaviors of PCy_3 with $W_6S_8(4\text{-tbp})_6$ (**4**) and $W_6S_8(n\text{-butylamine})_6$ (**2**) are different, i.e., $W_6S_8(PCy_3)_6$ (**3**) is formed in the latter case, but *cis*-$W_6S_8(PCy_3)_4(4\text{-tbp})_2$ (**1**) is formed in the former. This could be due to the difference in the binding energies of 4-tbp and *n*-butylamine ligands. The different behavior might also be explained by the different volumes of the ligands: 4-tbp ligand is larger than *n*-butylamine. When four PCy_3 ligands are bound to the W_6S_8 cluster, the axial ligand environment is already quite crowded, as easily seen in the crystal structure. The reaction rate of the bulky phosphine ligand with sterically hindered structure maybe slower, as observed previously in some single metal complexes.[37] The substitution reaction seems to be kinetically trapped in the sterically hindered stage of *cis*-$W_6S_8(PCy_3)_4(4\text{-tbp})_2$ under the conditions reported here. In fact, if the reaction were pushed hard enough by adding 6 equiv more of PCy_3, $W_6S_8(PCy_3)_6$ is the ultimate product even if starting with $W_6S_8(tbp)_6$.

Properties of *cis*-$W_6S_8(PCy_3)_4$(4-*tert*-butylpyridine)$_2$ (1). Although **1** is not the most desirable complex for low-dimensional linking, it is *possible* to use it as a precursor for a zigzag 1-D chain or "molecular square"[39] of clusters, etc. Research is underway toward building multicluster complexes using this compound. Some preliminary observations of its properties are reported here.

Pure *cis*-$W_6S_8(PCy_3)_4(4\text{-tbp})_2$ (**1**) complex was heated at 100 °C for 1 day in benzene to see whether it isomerizes and reaches equilibrium with other possible complexes in the series. Intra and/or inter PCy_3 ligand exchange occurred under this condition, and other complexes were observed, which is not conducive to the planned linking reactions. Similar reactions run at lower temperatures (70 and 40 °C) also showed this rearrangement but with slower rates. This phenomenon was used to make an educated guess concerning the assignments of the new ^{31}P NMR peaks, and the distribution of other complexes in the series was calculated (see section C). An amount of 74% of **1** was still present after 1 day at 100 °C. This is the same as the yield of **1** in the 1:4 reaction in THF as previously described, indicating that this is an equilibrium result. We found the ratio of *trans*-$W_6S_8(PCy_3)_4(4\text{-tbp})_2$ (4.4%) to *cis*-$W_6S_8(PCy_3)_4(4\text{-tbp})_2$ (74%) to be 1:17, which is much smaller than the ratio of 1:4 if only a statistical distribution is assumed. Also, a purely statistical distribution of four PR_3 and two 4-tbp ligands would result in 26.3% *cis*-$W_6S_8(PR_3)_4(4\text{-tbp})_2$. Both of these observations show that this *cis*-$W_6S_8(PCy_3)_4(4\text{-tbp})_2$ complex is energetically favored. However, because of the partial loss of the "preprogrammed" cis configuration, caution needs to be taken when using this compound as a precursor for linking reactions.

Ligand Exchange Reaction of W_6S_8(4-*tert*-butylpyridine)$_6$ with *n*-Butylamine. $W_6S_8(n\text{-butylamine})_6$ (**2**) was used as a springboard to the $W_6S_8(PCy_3)_6$ (**3**) cluster, but it is also of general interest because understanding the lability of the different ligands on W_6S_8 clusters builds up a suitable material base for cluster linking. Primary amines such as *n*-propylamine were examined by McCarley and co-workers in their $Mo_6S_8L_6$ cluster syntheses from Mo_6Cl_{12}.[13] A large excess of *n*-butylamine is needed to completely substitute the 4-tbp, and the substitution is extremely slow at room temperature. In fact, the $W_6S_8(tbp)_6$ cluster is insoluble in cold *n*-butylamine. The current reaction uses about a 20-fold excess of amine to 4-tbp ligand at 100 °C. On the basis of the comparison of TGA results, *n*-butylamine is a more labile ligand than piperidine and tbp,[20] which makes it a good precursor to other clusters, as in the facile synthesis of cluster **3**.

Ligand Substitution Reaction of $W_6S_8(n\text{-butylamine})_6$ (2) with PCy_3. Since PCy_3 is thermodynamically more favorable than the *n*-butylamine ligand, it is easy to replace *n*-butylamine with PCy_3. Stoichiometric amounts (1:6) of PCy_3 fully replace the *n*-butylamine ligands on **2**. Using less than 6 equiv of PCy_3 yielded green solutions that were mixtures of $W_6S_8(n\text{-butylamine})_{6-n}(PCy_3)_n$, but the dominance of some complexes like *cis*-$W_6S_8(PCy_3)_4(4\text{-tbp})_2$ in the tbp cluster case was not observed in either THF or benzene.

The existence of the $W_6S_8(PCy_3)_6$ cluster is very interesting—even though PCy_3 is bulky, it is still possible to accommodate all six of them in the outer ligand sphere by adjusting the conformations and meshing them into each other. The longer W−P bond length compared with that found in the $W_6S_8(PEt_3)_6$ cluster and the lower decomposition temperature observed in the TGA experiments suggest that there is some steric repulsion between the Cy groups and S atoms on the cluster faces. However, PCy_3 is still thermodynamically more favorable than the 4-tbp ligand—neat 4-tbp failed to fully replace the PCy_3 at 100 °C.

B. Crystal Structures. All molecular structures described here can be summarized as $W_6S_8(LL')_6$. They share the same W_6S_8 core structure, which can be described as an octahedron of tungsten atoms with their octahedral faces capped by eight triply bridging sulfur atoms. Variations come from different axial ligands L and small differences in the W_6S_8 core structure caused by different ligand environments. Complex **1** has an unusual distorted cluster core. Selected data are presented in Tables 2, 3, and 4 for clusters **1**, **2**, and **3**, respectively, and the structural comparison between these and other previously reported $W_6S_8L_6$ clusters is presented in Table 5.

***cis*-$W_6S_8(PCy_3)_4$(4-*tert*-butylpyridine)$_2$ (1)·2 heptane.** To our knowledge, this is the first reported group 6 neutral octahedral metal chalcogenide cluster with mixed axial ligands. The crystal structure consists of four discrete *cis*-$W_6S_8(PCy_3)_4(4\text{-tbp})_2$ molecules sitting on the 2-fold axes of the C-center monoclinic cell. The molecular structure of **1** is shown in Figure 1.

The average W−W distance is 2.680 Å, larger than the average W−W distance of 2.662 Å seen in $W_6S_8(4\text{-tbp})_6$[19] and shorter than in $W_6S_8(PCy_3)_6$, 2.683 Å, but much closer to the latter. The average W−S distance is 2.454 Å, close to those of other W_6S_8 clusters. The new feature is that the cluster has two 4-tbp and four bulky PCy_3 axial ligands. Since neutral chalcogenide octahedral clusters with mixed ligands were not known before, it is worth examining the structure in detail. Figure 2 shows the bare cluster core and only the coordinating N and P atoms. The deviations in bond lengths and bond angles in this W_6S_8 core structure are significantly greater than in any W_6S_8 clusters with uniform axial ligands. The W−W distances in **1** range from 2.657 to 2.710 Å with a δ (maximum deviation) of 0.053 Å (2% of the average W−W distance) compared with the largest δ of 0.021 Å $W_6S_8L_6$ clusters (see Table 5). The W−W−W angles within equatorial squares range from 89.189° to 91.068° with an average of 89.997° and δ of 1.88° (2% of the average angle). The maximum deviation of these angles in other $W_6S_8L_6$ clusters is 0.4° at most. However, amidst all these deviations in W atom positions, the W−S distances are nearly

(39) Stang, P. J.; Olenyuk, B. *Acc. Chem. Res.* **1997**, *30*, 502−518.

Table 2. Selected Bond Lengths [Å] and Angles [deg] for *cis*-$W_6S_8(PCy_3)_4$(4-*tert*-butylpyridine)$_2$[a]

W(1)−W(2)	2.6886(3)	W(1)−S(2)A	2.4422(12)
W(1)−W(3)	2.6701(3)	W(1)−S(2)	2.4437(11)
W(1)−W(1)A	2.6928(3)	W(1)−S(4)	2.4538(11)
W(1)−W(2)A	2.7099(3)	W(1)−S(1)	2.4586(12)
W(2)−W(3)	2.6768(3)	W(2)−S(4)A	2.4427(11)
W(2)−W(3)A	2.6573(3)	W(2)−S(1)	2.4506(11)
W(3)−W(3)A	2.6648(4)	W(2)−S(2)	2.4589(12)
		W(2)−S(3)	2.4801(13)
W(1)−P(1)	2.5960(12)	W(3)−S(1)	2.4444(12)
W(2)−P(2)	2.6037(12)	W(3)−S(4)	2.4481(11)
W(3)−N(1)	2.259(4)	W(3)−S(3)	2.4562(12)
		W(3)−S(3)A	2.4671(12)
W(3)−W(1)−W(1)A	89.693(5)		
W(1)−W(3)−W(3)A	90.294(5)	W(1)−S(2)−W(1)A	66.89(3)
W(2)−W(1)−W(2)A	89.684(9)	W(1)−S(2)−W(2)	66.52(3)
W(1)−W(2)−W(3)A	90.054(8)	W(2)−S(2)−W(1)A	67.13(3)
W(3)−W(2)−W(1)A	89.189(7)	W(2)−S(3)−W(3)	65.68(3)
W(2)−W(3)−W(2)A	91.067(9)	W(2)−S(3)−W(3)A	64.98(3)
		W(3)−S(3)−W(3)A	65.54(3)
W(3)−W(1)−W(2)	59.936(7)	W(1)−S(4)−W(3)	66.01(3)
W(1)−W(2)−W(3)	59.688(6)	W(1)−S(4)−W(2)A	67.20(3)
W(1)−W(3)−W(2)	60.376(7)	W(3)−S(4)−W(2)A	65.82(3)
W(3)−W(1)−W(2)A	59.193(7)		
W(1)−W(2)A−W(3)	59.658(7)	S(1)−W(1)−S(2)	90.64(4)
W(1)−W(3)−W(2)A	61.149(7)	S(1)−W(1)−S(4)	89.93(4)
W(3)−W(2)−W(3)A	59.942(8)	S(2)−W(1)−S(2)A	89.60(5)
W(2)−W(3)−W(3)A	59.665(7)	S(4)−W(1)−S(2)A	88.59(4)
W(2)−W(3)A−W(3)	60.392(7)	S(1)−W(2)−S(2)	90.47(4)
W(1)−W(2)−W(1)A	59.840(8)	S(1)−W(2)−S(3)	88.77(4)
W(2)−W(1)−W(1)A	60.472(7)	S(2)−W(2)−S(4)A	88.46(4)
W(2)−W(1)A−W(1)	59.688(7)	S(3)−W(2)−S(4)A	91.11(4)
		S(1)−W(3)−S(3)	89.46(4)
W(1)−S(1)−W(2)	66.41(3)	S(1)−W(3)−S(4)	90.40(4)
W(1)−S(1)−W(3)	65.99(3)	S(3)−W(3)−S(3)A	88.15(5)
W(2)−S(1)−W(3)	66.30(3)	S(4)−W(3)−S(3)A	91.29(4)

[a] Symmetry transformations used to generate equivalent atoms: A, $-x + 2, y, -z + {}^1/_2$.

Table 3. Selected Bond Lengths [Å] and Angles [deg] for W_6S_8(*n*-butylamine)$_6$[a]

W(1)−W(2)	2.659(2)	W(1)−S(1)	2.459(13)
W(1)−W(2)B	2.655(2)	W(1)−S(2)	2.446(14)
W(2)−W(2)B	2.648(3)	W(1)−S(3)B	2.461(10)
W(2)−W(2)C	2.651(3)	W(2)−S(1)	2.463(10)
		W(2)−S(3)	2.447(9)
W(1)−N(1)	2.22(5)	W(2)−S(3)B	2.430(10)
W(2)−N(2)	2.29(4)	W(2)−S(2)A	2.474(12)
		W(1)−S(2)−W(2)B	65.3(3)
W(2)−W(1)−W(2)A	89.70(7)	W(2)A−S(2)−W(2)B	64.8(4)
W(1)−W(2)−W(1)A	90.30(7)	W(2)−S(3)−W(2)B	65.8(2)
		W(2)B−S(3)−W(1)A	65.8(2)
W(2)−W(1)−W(2)B	59.80(7)	W(2)−S(3)−W(1)A	65.5(2)
W(1)−W(2)−W(2)B	60.03(6)		
W(1)−W(2)B−W(2)	60.18(6)	S(1)−W(1)−S(3)B	89.3(2)
W(1)−W(2)−W(2)C	60.09(4)	S(2)−W(1)−S(3)B	90.3(2)
W(2)−W(1)−W(2)C	59.81(7)	S(1)−W(1)−S(2)	173.9(4)
W(2)−W(1)A−W(2)C	59.91(7)	S(3)A−W(1)−S(3)B	171.8(5)
W(2)C−W(2)−W(1)A	60.04(4)	S(3)−W(2)−S(3)B	88.9(4)
		S(1)−W(2)−S(3)B	89.9(4)
		S(1)−W(2)−S(2)A	90.5(4)
W(1)−S(1)−W(2)	65.4(3)	S(1)−W(2)−S(3)	173.2(3)
W(2)−S(1)−W(2)C	65.1(3)	S(2)A−W(2)−S(3)B	173.6(3)

[a] Symmetry transformations used to generate equivalent atoms: B, $-x - 2, y, -z + 1$; A, $-x - 2, -y + 1, -z + 1$; C, $x, -y + 1, z$.

unaffected, ranging from 2.442 to 2.480 Å with a δ of 0.038 Å, even smaller than the respective δ in some other clusters. A closer look at those unequal bond lengths and angles reveals that the shortest W−W distance is not between the W atoms with 4-tbp as ligands, namely, W3 and W3A, but between W2 and W3A (or symmetry equivalent W2A and W3). The longest

Table 4. Selected Bond Lengths [Å] and Angles [deg] for $W_6S_8(PCy_3)_6$[a]

W(1)−W(2)	2.6806(5)	W(1)−S(1)	2.458(2)
W(1)−W(2)#1	2.6832(5)	W(1)−S(2)	2.451(2)
W(1)−W(3)	2.6842(5)	W(1)−S(3)	2.446(2)
W(1)−W(3)#1	2.6863(4)	W(1)−S(4)	2.445(2)
W(2)−W(3)	2.6821(4)	W(2)−S(1)	2.446(2)
W(2)−W(3)#1	2.6861(4)	W(2)−S(2)	2.456(2)
		W(2)−S(3)A	2.451(2)
W(1)−P(1)	2.604(3)	W(2)−S(4)A	2.445(2)
W(2)−P(2)	2.593(2)	W(3)−S(1)	2.450(2)
W(3)−P(3)	2.614(2)	W(3)−S(2)A	2.451(2)
		W(3)−S(3)	2.455(2)
		W(3)−S(4)A	2.442(2)
W(1)−W(3)−W(1)A	89.906(14)		
W(3)−W(1)−W(3)A	90.094(14)	W(1)−S(3)−W(2)A	66.45(5)
W(2)−W(3)−W(2)A	89.855(13)	W(1)−S(3)−W(3)	66.43(5)
W(3)−W(2)−W(3)A	90.145(13)	W(2)A−S(3)−W(3)	66.39(5)
W(1)−W(2)−W(1)A	90.051(14)	W(3)A−S(4)−W(2)A	66.57(5)
W(2)−W(1)−W(2)A	89.949(14)	W(3)A−S(4)−W(1)	66.68(5)
		W(2)A−S(4)−W(1)	66.55(5)
W(1)−W(2)−W(3)	60.071(12)		
W(2)−W(3)−W(1)	59.937(12)	S(4)−W(1)−S(3)	89.67(7)
W(3)−W(1)−W(2)	59.992(12)	S(4)−W(1)−S(2)	89.51(7)
W(1)−W(2)−W(3)A	60.073(12)	S(3)−W(1)−S(2)	172.27(7)
W(2)−W(3)A−W(1)	59.862(12)	S(4)−W(1)−S(1)	171.85(7)
W(3)A−W(1)−W(2)	60.065(12)	S(3)−W(1)−S(1)	89.91(7)
W(1)−W(2)A−W(3)	59.990(12)	S(2)−W(1)−S(1)	89.81(7)
W(2)A−W(3)−W(1)	59.951(12)	S(4)A−W(2)−S(1)	89.58(7)
W(3)C−W(1)−W(2)A	60.059(12)	S(4)A−W(2)−S(3)A	89.55(7)
W(1)A−W(2)−W(3)	60.091(12)	S(1)−W(2)−S(3)A	172.36(7)
W(2)−W(3)−W(1)A	59.975(12)	S(4)A−W(2)−S(2)	171.96(7)
W(3)−W(1)A−W(2)	59.935(12)	S(1)−W(2)−S(2)	89.98(7)
		S(3)A−W(2)−S(2)	89.82(7)
W(2)−S(1)−W(3)	66.43(6)	S(4)A−W(3)−S(1)	89.55(7)
W(2)−S(1)−W(1)	66.26(5)	S(4)A−W(3)−S(2)A	89.58(7)
W(3)−S(1)−W(1)	66.30(5)	S(1)−W(3)−S(2)A	172.16(7)
W(3)A−S(2)−W(1)	66.45(5)	S(4)A−W(3)−S(3)	171.75(7)
W(3)A−S(2)−W(2)	66.37(6)	S(1)−W(3)−S(3)	89.90(7)
W(1)−S(2)−W(2)	66.22(5)	S(2)A−W(3)−S(3)	89.85(7)

[a] Symmetry transformations used to generate equivalent atoms: A, $-x, -y + 1, -z + 1$.

W−W distance is not between those W atoms trans to the 4-tbp ligands, namely, W1−W1A, but between W2 and W1A (or symmetry equivalent W2A and W1). The average W−W distance on the front triangular face of W2−W3−W3A is shorter than the average W−W distance on the back triangular face of W2−W1−W1A by 0.03 Å. In fact, the former are the three shortest W−W distances and the latter the three longest ones. In the W−W−W angles within the equatorial square of W1−W1A−W3A−W3, the angle is less than 90° in the back and more than 90° in the front. We conclude that W2 and W2A are distorted out of the ideal octahedral positions and pushed toward W3 and W3A, respectively.

The distortion above may be explained by the distortion in the ligand environment due to steric interactions. All W−L distances are comparable to analogous clusters; the W−N distance is 2.259 Å, very close to 2.257 Å in W_6S_8(4-tbp)$_6$, and the mean W−P distance is 2.600 Å, also close to 2.604 Å in $W_6S_8(PCy_3)_6$. However, the L−L distances are quite different; the N−N distance between the two 4-tbp ligands here is 6.120 Å, much longer than those in W_6S_8(4-tbp)$_6$ cluster, 5.789−5.917 Å;[4] the P1−P1A distance is 6.707 Å, 0.3 Å larger than those P−P distances in $W_6S_8(PCy_3)_6$. As Saito observed, the L−L distances are sensitive to distortions in ligand environments, and distortions in the cluster core often parallel the distortions in ligand environments.[4] Apparently, the two 4-tbp ligands are "opened up" a little bit to accommodate the bulky PCy_3 groups squeezing in from the top and bottom (illustrated with the arrows

Table 5. Summary of Selected Interatomic Distances [Å] and Bond Angles [deg] for $W_6S_8(LL')_6$ Clusters[a]

clusters	$W_6S_8(PEt_3)_6$	$W_6S_8(PCy_3)_6$	*cis*-$W_6S_8(PCy_3)_4(tbp)_2$	W_6S_8(4-tbp)$_6$	$W_6S_8(py)_6$	$W_6S_8(pip)_6$	W_6S_8(*n*-butylamine)$_6$
W−W	2.678−2.681	2.681−2.686	2.657−2.710	2.656−2.667	2.654−2.667	2.653−2.674	2.648−2.659
mean	2.680	2.684	2.680	2.662	2.662	2.666	2.655
δ_{w-w}	0.003	0.06	0.053	0.011	0.011	0.021	0.011
BO(PBO)[b]	0.841 (1.01)	0.829 (0.994)	0.841 (1.01)	0.902 (1.08)	0.902 (1.08)	0.888(1.06)	0.926(1.15)
W−S	2.436−2.472	2.442−2.458	2.442−2.480	2.457−2.469	2.430−2.478	2.441−2.478	2.430−2.474
mean	2.458	2.450	2.454	2.461	2.456	2.462	2.455
δ_{w-s}	0.036	0.016	0.038	0.012	0.048	0.037	0.044
W−W−W[c]	89.93−90.07	89.86−90.15	89.19−91.07	90.0−90.0	89.8−90.2	89.77−90.22	89.70−90.30
mean	90.00	90.00	89.96	90.0	90.0	90.00	90.00
δ_{w-w-w}	0.14	0.29	1.88	0.0	0.4	0.55	0.60
W−W−W[d]	59.94−60.05	59.86−60.09	59.19−61.15	59.9−60.3	59.7−60.2	59.53−60.30	59.80−60.18
δ_{w-w-w}	0.11	0.229	1.96	0.4	0.5	0.77	0.38
W−L	2.518−2.525	2.593−2.614	P:2.596, 2.604 N: 2.259	2.257	2.257−2.275	2.310−2.315	2.22−2.29
mean	2.521	2.604	P: 2.600	2.257	2.263	2.312	2.27
L−L	6.174−6.310	6.311−6.406	P:6.333−6.707 N: 6.120	5.789−5.917	5.748−5.932	5.756−6.100	5.827−5.918
δ_{L-L}	0.136	0.095	P: 0.374	0.128	0.184	0.346	0.091
space groups[e]	$P\bar{1}$, ($R\bar{3}$)	$P\bar{1}$	$C2/c$, ($P2_1$)	$R\bar{3}$, ($C2/c$ and $P\bar{1}$)	$P\bar{1}$	$I\bar{4}$	$C2/m$
ref[f]	18, (20)	herein	herein	19, (20)	19, (21)	20	herein

[a] Some data were taken from ref 4. [b] BO (bond order) n is defined as: $d(n) = d(1) - 0.6 \log n$; $d(1) = 2.635$ Å for W; PBO (Pauling bond order) $= n \times 4/(20/6)$. [c] Within equatorial squares. [d] Within triangular faces. The mean angles are 60° by geometry. [e] All the space groups reported to occur for the clusters. Only the data from one of each cluster are shown, the others are in parentheses. [f] The references in which the shown data were reported are outside of parentheses. Three clusters are reported herein.

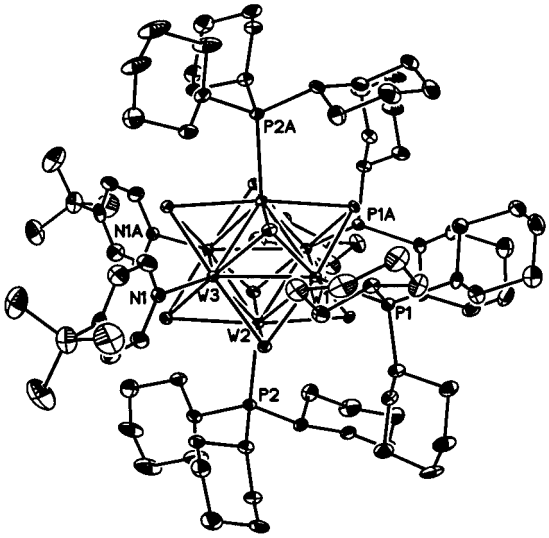

Figure 1. ORTEP drawing of *cis*-$W_6S_8(PCy_3)_4$(4-tbp)$_2$ (**1**) cluster at 40% probability level.

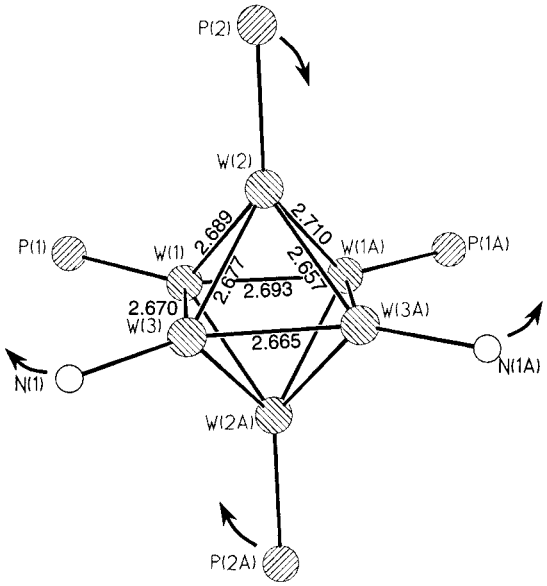

Figure 2. Core structure of *cis*-$W_6S_8(PCy_3)_4$(4-tbp)$_2$ (**1**) cluster with S and C atoms omitted for clarity.

in Figure 2), which is a natural way of releasing the steric hindrance caused by four bulky PCy_3 ligands. These axial ligand distortions "drag" the corresponding core W atoms accordingly, causing the distortion in cluster core described above. This might be the best way to keep all the ligands together in this crowded structure, surely better than the alternative *trans*-$W_6S_8(PCy_3)_4$-(4-tbp)$_2$, in which PCy_3 ligands have to inevitably coexist uncomfortably on the four equatorial positions.

W_6S_8(*n*-butylamine)$_6$ (2). The structures of the octahedral chalcogenide clusters with primary amine ligands have been pursued for some time. McCarley and co-workers reported that the possible Mo_6S_8(*n*-propylamine)$_6$ crystal was glassy.[13] W_6S_8-(*n*-hexylamine)$_6$, which has been synthesized in this lab previously, was very hard to crystallize possibly because of the long "greasy" hexyl chain. It was found that this fragile crystal of **2** became glassy and opaque after a few hours out of the mother liquid and that the crystals became polycrystalline in polybutene oil in a cold N_2 stream. Sealing the crystal in a capillary with the mother liquid allowed an acceptable data set to be acquired. The solved structure is shown in Figure 3.

This structure finally answered the question about the existence and stability of a primary amine W_6S_8 cluster and provided some information about the ligand's binding strength. Cluster **2** has the shortest W−W distance (2.655 Å) among $W_6S_8L_6$ clusters, but the W−N (2.27 Å) distance is not significantly different from those in W_6S_8(4-tbp)$_6$ (2.257 Å) and $W_6S_8(py)_6$ (2.263 Å) based on the current mediocre structure refinements.

$W_6S_8(PCy_3)_6$ (3)·2 heptane. The crystal structure contains one spherelike **3** cluster sitting on the inversion center of a triclinic cell with two heptane molecules in the cavities between clusters. As shown in Figure 4, the cluster is highly crowded like a solid sphere, with the compact nonpolar outer ligand layer almost completely covering up the inner cluster core as shown in a space-filling model of this cluster structure in Figure 5.

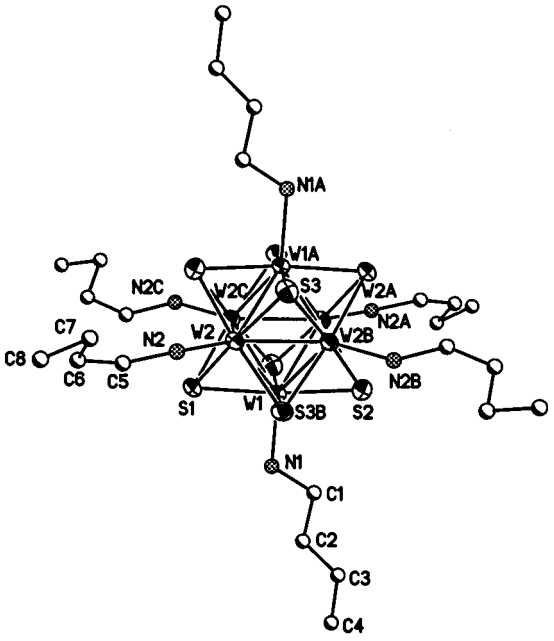

Figure 3. Molecular structure of W_6S_8(*n*-butylamine)$_6$ (**2**) cluster. Atoms with thermal ellipsoids are at 30% probability level.

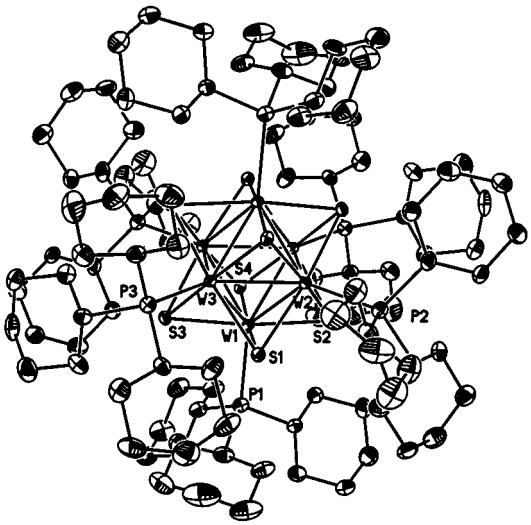

Figure 4. ORTEP drawing of $W_6S_8(PCy_3)_6$ (**3**) cluster at 40% probability level.

The average W−W interatomic distance in **3** is 2.684 Å, comparable to but a little longer than that in the $W_6S_8(PEt_3)_6$ cluster, 2.680 Å.[18] The cluster is quite regular as indicated by the small deviations δ_{w-w} and δ_{p-p}. The average W−P distance, 2.604 Å, is significantly longer than the W−P distance in $W_6S_8(PEt_3)_6$ cluster, 2.522 Å.[18] This might be explained by the steric hindrance in the outer ligand sphere. The W−P bonds are stretched a little bit to accommodate the bulky PCy_3 better.

It is intriguing to observe how the cyclohexyl groups on PCy_3 are cleverly arranged on the spherical surface. Every cyclohexyl group points toward and "meshes" between two cyclohexyl groups on the neighboring ligands, thus avoiding unnecessary bumping with each other. This "intermeshing" of the ligands greatly decreases the steric hindrance in this seemingly impossible structure. This might also account for its low solubility in most solvents because the restricted conformation by the interlocked ligands leads to poor interactions with solvent molecules.

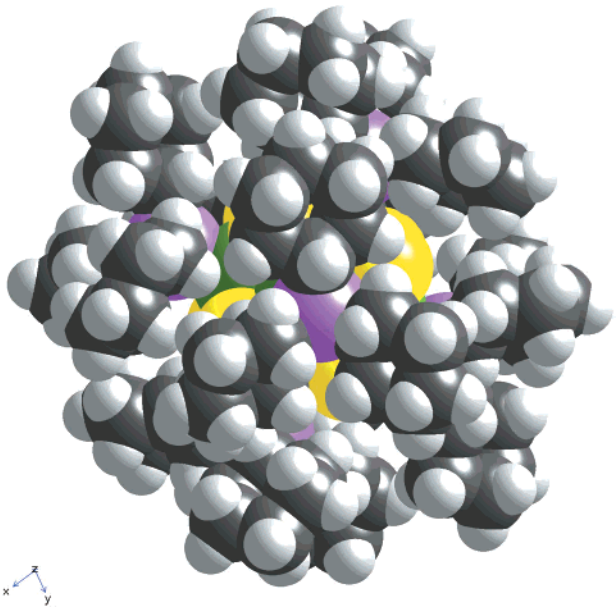

Figure 5. Space filling representation of $W_6S_8(PCy_3)_6$ (**3**) cluster. Color code and radii are the following: W, green, 1.87 Å; S, yellow, 1.53 Å; P, purple, 1.60 Å; C, gray, 1.27 Å; H, silver, 0.82 Å.

C. NMR Spectroscopy of Cluster Complexes $W_6S_8(PCy_3)_n(4\text{-tbp})_{6-n}$ ($0 < n < 6$). (a) ^{1}H and ^{31}P NMR of *cis*-$W_6S_8(PCy_3)_4(4\text{-tbp})_2$ (1). ^{1}H NMR and ^{31}P NMR spectra were collected for complex **1**. The H resonances on 4-tbp of *cis*-$W_6S_8(PCy_3)_4$(4-*tert*-butylpyridine)$_2$ are shifted from the ones of the W_6S_8(4-tbp)$_6$ cluster.[20] The signals from H on PCy_3 ligands are very broad bands that are different from free PCy_3 but not illuminating. We hoped to utilize the ^{1}H NMR to identify the complexes $W_6S_8(4\text{-tbp})_{6-n}(PR_3)_n$ ($0 < n < 6$). In fact, they are helpful based on the different numbers of equivalent 4-tbp ligands and their ratios (see Table 6), *if* individual cluster complexes are isolated. It also appeared that the more phosphines on the cluster, the more upfield the chemical shifts of the H on the 4-tbp ligands are. However, these peaks are all cramped into a small range from 9.9 to 9.5 ppm (in C_6D_6) and overlapped with each other. They are not easily distinguishable from one another in mixtures of complexes.

What is more interesting and useful is the ^{31}P{^{1}H} NMR of complex **1**, shown in Figure 6A. Although ^{31}P NMR has been employed before in the studies of octahedral cluster complexes and proven to be very useful,[30,31,33,40] the new features observed in ^{31}P NMR of $W_6S_8(4\text{-tbp})_{6-n}(PR_3)_n$ allows in situ cluster identification. First, some of these complexes have chemically inequivalent phosphines. In the case of complex **1**, the two big peaks with equal intensities in Figure 6A can be readily explained by two kinds of chemically inequivalent P atoms, each including two chemically equivalent P atoms per cluster, namely, P1, P1A and P2, P2A in the crystal structure. Second, the broad satellite peaks symmetrically positioned around each of the main peaks are due to the coupling to the NMR active ^{183}W isotope ($I = {}^1/_2$). The intensities of a pair of satellites relative to their main peak intensity are in agreement with the 14.4% natural abundance of ^{183}W.[41] And the coupling constant $^1J_{W-P}$, about 200 Hz, is reasonable.[42] Finally, the triplet splitting of each peak

(40) (a) Imoto, H.; Hayakawa, S.; Morita, N.; Saito, T. *Inorg. Chem.* **1990**, *29*, 2007−2014. (b) Saito, T.; Nishida, M.; Yamagata, T. *Inorg. Chem.* **1986**, *25*, 1111−1117.
(41) Harris, R. K. In *NMR and the Periodic Table*; Harris, R. K., Mann, B. E., Eds.; Academic Press: New York, 1978.

Table 6. Numbers, Ratios, and Couplings of ^{31}P and ^{1}H NMR Peaks for $W_6S_8(PR_3)_n(4\text{-tbp})_{6-n}$[a]

n	*Isomers*	Structure Diagrams[b]	^{31}P NMR			^{1}H NMR[c]		Notes[d]
			No. of Peaks	Ratios and Couplings	Satellite Peaks	No. of Peaks	Ratios	
1			1	singlet	singlet	2	4:1	*H*
2	*trans*		1	singlet	singlet	1		*H*
	cis		1	singlet	doublet	2	1:1	*H,S*
3	*fac*		1	singlet	triplet	1		*S*
	mer		2	2:1 doublet:triplet		2	2:1	*P,H*
4	*cis*		2	1:1 triplet:triplet		1		*P*
	trans		1	singlet		1		
5			2	4:1 doublet:quintet		1		*P*
6			1	singlet		0		*H*

[a] $n = 1-6$. [b] The cage structure represents W_6S_8 cluster; P = PR_3 ligand; empty sites are occupied by 4-tbp. [c] The peaks from α-Hs on pyridine ring of 4-tbp ligands. [d] "*P*" means that it can be identified with ^{31}P coupling patterns. "*S*" means that it can be identified with ^{31}P satellite peak patterns. "*H*" means that it can be identified with ^{1}H NMR if isolated. The rest can be identified by chemical shifts and mass balance.

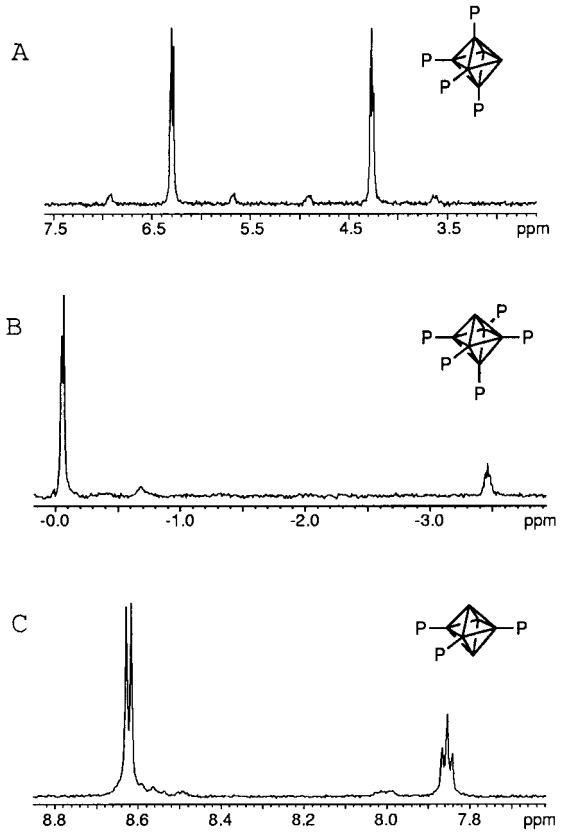

Figure 6. ^{31}P NMR spectra of selected $W_6S_8(PCy_3)_{6-n}(tbp)_n$ complexes with P−P coupling (in C_6D_6 referenced to 85% H_3PO_4): (A) pure *cis*-$W_6S_8(PCy_3)_4(4\text{-tbp})_2$ (**1**) cluster; (B) $W_6S_8(PCy_3)_5(4\text{-tbp})$ cluster; (C) *mer*-$W_6S_8(PCy_3)_3(4\text{-tbp})_3$ cluster. Parts B and C are magnified portions from a ^{31}P NMR spectrum of a mixture.

can only be explained by the coupling between the inequivalent P atoms. Besides W, P, and H (decoupled), other atoms present in cluster complex either do not have NMR active isotopes (S) or do not have significant abundance for the NMR active isotopes (C and N).[41] Although P−P coupling via three bonds is very uncommon,[42] it has been observed in metal chloride clusters containing multiple bonds with even larger coupling constants[43−45] and in some chalcogenide clusters.[46,47] However, it has not been reported for octahedral metal clusters before. The equal coupling constants ($^3J_{P-P} = 2.4$ Hz) for the two triplets and two equivalent P atoms for each kind of inequivalent P atom fit the "double triplets" picture.

(b) P−P Coupling in Other $W_6S_8(PCy_3)_n(4\text{-tbp})_{6-n}$ ($0 < n < 6$) Complexes. If the triplet splitting is truly caused by P−P coupling, we should see the analogous P−P coupling in other cluster complexes with inequivalent phosphine ligands. As shown in Table 6, $W_6S_8(4\text{-tbp})(PR_3)_5$ should have a doublet:quintet splitting pattern with a 4:1 intensity ratio and *mer*-$W_6S_8(4\text{-tbp})_3(PR_3)_3$ should have a doublet:triplet pattern with a 2:1 intensity ratio. Indeed, such peaks were observed in mixtures of $W_6S_8(4\text{-tbp})_{6-n}(PCy_3)_n$ complexes as shown in parts B and C of Figure 6, which were magnified from portions of a ^{31}P NMR spectrum of such a mixture. Examination of several mixtures revealed that the intensity ratios of these assumed coupled peaks followed the theoretically predicted values, while the ratios of other peaks varied from one mixture to another. The coupling constants $^3J_{P-P}$ are the same within experimental error, which is reasonable because of the expected small variations in the interatomic distances.

(c) P−P Coupling in the Isotopomers of $W_6S_8(PCy_3)_n(4\text{-tbp})_{6-n}$ ($0 < n < 6$) Complexes. Satellite peaks are generally broad because there are possible W isotopomers in which P atoms on different isotopic W atoms can lead to further P−P coupling even if they might be chemically equivalent based on their positions on the octahedra. This fine coupling is generally impossible to trace and observe for complexes with several phosphine ligands but possible for some simple cases. Figure 7 shows magnified $^{31}P\{H\}$ NMR of these $W_6S_8(PCy_3)_n(4\text{-tbp})_{6-n}$ complex mixtures, highlighting the fine coupling details of those satellites that can be practically predicted and observed. In $W_6S_8(tbp)_5(PCy_3)$, the only P atom is either bound to a ^{183}W (satellites) or not (main peak), so the satellites are singlets as shown in Figure 7A. In the case of *cis*-$W_6S_8(tbp)_4(PCy_3)_2$ (Figure 7B), isotopomer P−^{183}W−W−P (24.08% among all three isotopomers) gives doublet splitting on both satellite and main P peaks, which should dominate the satellite features because isotopomer P−^{183}W−^{183}W−P has a much lower probability (1.96%). For the slightly more complicated case of *fac*-$W_6S_8(tbp)_3(PCy_3)_3$, the satellite feature is dominated by isotopomer ^{183}W−W−W (31.65%), which leads to triplet splitting on satellites and a doublet on the main peak, as shown in Figure 7C.

(42) (a) Mason, J. In *Multinuclear NMR*; Mason, J., Ed.; Plenum Press: New York, 1987. (b) Minelli, M.; Enemark, J. H.; Brownlee, R. T. C.; O'Connor, M. J.; Wedd, A. G. *Coord. Chem. Rev.* **1985**, *68*, 169−278. (c) Pregosin, P. S.; Kunz, R. W. *Phosphorus-31 and Carbon-13 NMR of Transition Metal Phosphine Complexes*; Springer-Verlag: Berlin, 1979. (d) Verkade, J. G. *Coord. Chem. Rev.* **1972/1973**, *9*, 1−106. (e) See ref 41, chapter 8E.
(43) (a) Carlin, R. T. Ph.D. Thesis, Iowa State University, 1982. (b) Carlin, R. T.; McCarley, R. E. *Inorg. Chem.* **1989**, *28*, 3432−3436.
(44) Cotton, F. A.; Dikarev, E. V.; Wong, W.-Y. *Inorg. Chem.* **1997**, *36*, 3268−3276.
(45) Luck, R. L.; Morris, R. H.; Sawyer, J. F. *Inorg. Chem.* **1987**, *26*, 222.
(46) Cotton, F. A.; Kibala, P. A.; Matusz, M.; McCaleb, C. S.; Sandor, R. B. W. *Inorg. Chem.* **1989**, *28*, 2623−2630.
(47) Saito, T.; Kajitani, Y.; Yamagata, T.; Imoto, H. *Inorg. Chem.* **1990**, *29*, 2951−2955.

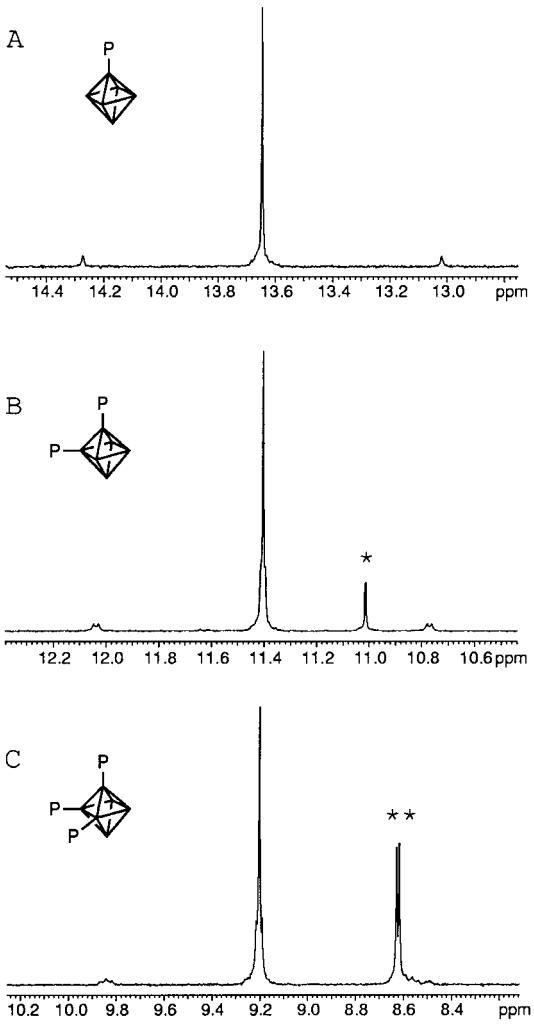

Figure 7. ^{31}P NMR spectra of selected $W_6S_8(PCy_3)_{6-n}(tbp)_n$ complexes highlighting fine P−P coupling in satellites (in C_6D_6 referenced to 85% H_3PO_4, portions from ^{31}P NMR spectrum of a mixture): (A) $W_6S_8(PCy_3)(4\text{-tbp})_5$; (B) *cis*-$W_6S_8(PCy_3)_2(4\text{-tbp})_4$ (∗ indicates *trans*-$W_6S_8(PCy_3)_2(4\text{-tbp})_4$); (C) *fac*-$W_6S_8(PCy_3)_3(4\text{-tbp})_3$ (∗∗ indicates the doublet from *fac*-$W_6S_8(PCy_3)_3(4\text{-tbp})_3$).

Since the ^{31}P NMR peaks are well separated from each other, these P−P coupling "fingerprints" are very useful in identifying and studying the specific cluster complexes *in the mixtures* even *before* we isolate and identify each individual complex. As noted in Table 6, three out of all nine complexes in this series can be unequivocally assigned by the main peak P−P coupling in the ^{31}P NMR. Two more complexes can be assigned with the coupling details in satellite peaks. If the species were isolated, ^{1}H NMR can differentiate $W_6S_8(tbp)_5(PR_3)$ and *trans*-$W_6S_8(4\text{-tbp})_4(PR_3)_2$ and identify $W_6S_8(PR_3)_6$. The only "featureless" complex, *trans*-$W_6S_8(4\text{-tbp})_2(PR_3)_4$, would account for the only unassigned peak.

However, chemical shift information for P atoms on different $W_6S_8(4\text{-tbp})_{6-n}(PR_3)_n$ has not been utilized yet. Since all the peaks are well separated, we can deduce the assignments of those less characteristic peaks as long as we know the starting stoichiometry. For instance, in the conversion reaction of complex **1**, the PCy_3 ligands on *cis*-$W_6S_8(PCy_3)_4(tbp)_2$ cluster rearranged to form other complexes not originally present. But conservation of mass requires that the total number of PCy_3 ligands remains constant. We assume an assignment and "normalize" the integrals of the peaks with the numbers of P atoms per cluster for each peak according to the tentative assignment. If we calculate the mass balance based on the "normalized" integrals of the proposed complexes, only the correct assignment can lead to a balance. With this method, the new peaks in this spectrum were assigned as 9.216 (s) from 3P of *fac*-$W_6S_8(PCy_3)_3(tbp)_3$ (5.3%), 8.635 (d) from 2P of *mer*-$W_6S_8(PCy_3)_3(tbp)_3$, 7.851 (t) from 1P of *mer*-$W_6S_8(PCy_3)_3(tbp)_3$, 4.774 (s) from 4P of *trans*-$W_6S_8(PCy_3)_4(tbp)_2$, −0.045 (d) from 4P of $W_6S_8(PCy_3)_5(tbp)$, −3.454 (quintet) from 1P of $W_6S_8(PCy_3)_5(tbp)$. Then the distribution of different cluster complexes after complex **1** was heated at 100 °C was determined as shown in parentheses: *fac*-$W_6S_8(PCy_3)_3(tbp)_3$ (5.3%), *mer*-$W_6S_8(PCy_3)_3(tbp)_3$ (5.7%), *trans*-$W_6S_8(PCy_3)_4(tbp)_2$ (4.4%), *cis*-$W_6S_8(PCy_3)_4(tbp)_2$ (73.6%), $W_6S_8(PCy_3)_5(tbp)$ (11%).

In summary, NMR spectroscopy, especially ^{31}P NMR spectroscopy, is a very powerful technique for identifying W_6S_8 complexes containing phosphine ligands and for monitoring "in situ" ligand substitution reactions involving phosphines even before isolating each species.

D. Thermogravimetric Analysis (TGA). The thermogravimetric analyses (TGA) of the clusters can give some approximate indication of the lability or binding strength of the ligands, though sometimes the TGA might be complicated by other factors such as high boiling points of the ligands. Among the new complexes reported herein, the decomposition temperature of $W_6S_8(PCy_3)_6$ (**3**) (indicated by the onset of weight loss) is the highest, 230 °C, comparable to that of $W_6S_8(PEt_3)_6$ cluster, 250 °C,[20] suggesting that PCy_3 is an inert ligand on W_6S_8 cluster. The decomposition temperature of W_6S_8(*n*-butylamine)$_6$ (**2**) is 100 °C, the lowest among the clusters investigated.[20] The TGA of *cis*-$W_6S_8(PCy_3)_4(tbp)_2$ (**2**) cluster is quite intriguing; with two distinctive decomposition temperatures, 100 and 190 °C, corresponding to the loss of 4-tbp and PCy_3 ligands, respectively, based on the weight composition. There is also a so far unexplained small weight gain around 180 °C, which persisted even after several samples were examined and TGA gas was changed to argon from N_2.

Conclusions

Substitution reactions of $W_6S_8L_6$ clusters with the bulky PCy_3 ligand were investigated to synthesize cluster complexes with mixed axial ligands for ultimate use in the low-dimensional cluster linking. *cis*-$W_6S_8(PCy_3)_4(tbp)_2$ cluster was produced preferentially and isolated readily when $W_6S_8(tbp)_6$ and 4−6 equiv of PCy_3 were used as the starting materials. The $W_6S_8(PCy_3)_6$ cluster was produced when W_6S_8(*n*-butylamine)$_6$ and 6 equiv of PCy_3 were used. Other conditions led to mixtures of $W_6S_8(PCy_3)_nL_{6-n}$ ($0 \le n \le 6$) complexes. *cis*-$W_6S_8(PCy_3)_4(tbp)_2$ has a distorted structure due to its mixed axial ligand environment. ^{31}P NMR of *cis*-$W_6S_8(PCy_3)_4(tbp)_2$ and other $W_6S_8(PR_3)_nL_{6-n}$ clusters revealed P−P coupling through three bonds, which is found to be extremely useful for identifying nearly all the $W_6S_8(PR_3)_nL_{6-n}$ cluster complexes in the mixture before the individual complexes are isolated.

Acknowledgment. This work was supported by the Department of Energy (Grant DE-FG02-87ER45298). This work made use of the Polymer Characterization Facility and Electron and Optical Microscopy Laboratory of the Cornell Center for Materials Research supported by NSF under Award DMR-9632275. We thank Dr. Emil Lobkovsky and Mr. Dave Fuller for their help in collecting the crystallographic data and the ^{31}P NMR spectra, respectively. Experimental assistance from our colleagues Jennifer Adamchuk, Laurie I. Hill, Lori L. Rayburn, and Ran Zhou is gratefully acknowledged.

Supporting Information Available: Lists of atomic positions and parameters, tables of bond lengths and angles for crystal structures of *cis*-$W_6S_8(PCy_3)_4$(4-*tert*-butylpyridine)$_2$·heptane, W_6S_8(*n*-butylamine)$_6$, and $W_6S_8(PCy_3)_6$·2 heptane, thermogravimetric traces of *cis*-$W_6S_8(PCy_3)_4$(4-*tert*-butylpyridine)$_2$, W_6S_8(*n*-butylamine)$_6$, and $W_6S_8(PCy_3)_6$ clusters, examples of $^{31}P\{^1H\}$ NMR spectra of a mixture of $W_6S_8(PCy_3)_n(tbp)_{6-n}$ cluster complexes, and X-ray crystallographic files in CIF format for the structure determinations of *cis*-$W_6S_8(PCy_3)_4$(4-*tert*-butylpyridine)$_2$·heptane, W_6S_8(*n*-butylamine)$_6$, and $W_6S_8(PCy_3)_6$·2 heptane. This material is available free of charge via the Internet at http://pubs.acs.org.

IC991426L